Stability of Main-Group Element-Centered Gold Cluster Cations

Oliver D. Häberlen,† Hubert Schmidbaur,‡ and Notker Rösch*,†

Contribution from the Lehrstuhl für Theoretische Chemie and Anorganisch-Chemisches Institut, Technische Universität München, D-85747 Garching, Germany

Received February 22, 1994®

Abstract: Relativistic electronic structure calculations have been carried out for the main-group element-centered octahedral gold cluster cations $[(LAu)_6X_m]^{m+}$ (with central atoms X_1 = B, X_2 = C, and X_3 = N and ligands L = PH_3 or $P(CH_3)_3$) as well as for the corresponding series of four- and five-coordinate element-centered cations $[(LAu)_4X_m]^{(m-2)+}$ and $[(LAu)_5X_m]^{(m-1)+}$. Geometry optimization shows that the phosphine-ligated clusters have an X–Au bond which, on the average, is about 4 pm larger than that of the analogous naked clusters; the corresponding force constant is concomitantly weaker. The contribution of the ligands to the overall stability of the clusters is significant, as the cluster cations are stabilized more the higher the cluster charge; the effect is even more pronounced for trimethylphosphine ligands. When the central atom of the naked cluster core is varied, an opposite trend is found as the cluster stability decreases along the series B → C → N. Both effects compounded lead to a maximum of stability for the cluster cations $[(AuL)_4N]^+$, $[(AuL)_5C]^+$, and $[(AuL)_6C]^{2+}$, in agreement with the experimental results. Furthermore, all ligated octahedral clusters are calculated to be stable with respect to the loss of an AuL^+ moiety while the corresponding reaction leading to a five-coordinate cluster core is energetically feasible for the naked metal clusters. Thus the study of ligand-free models is not meaningful for an analysis of the electronic structure of gold phosphine compounds.

1. Introduction

In recent years a wide variety of higher coordinated main-group element-centered gold cluster cations have been synthesized,[1] e.g. the four-coordinate tetrahedral $[(LAu)_4N]^+$ [2] and square-pyramidal $[(LAu)_4As]^+$ [3] clusters, the five-coordinate trigonal bipyramidal clusters $[(LAu)_5C]^+$,[4] $[(LAu)_5N]^{2+}$,[5] and $[(LAu)_5P]^{2+}$,[6] and the six-coordinate octahedral clusters $[(LAu)_6C]^{2+}$ [7] and $[(LAu)_6P]^{3+}$.[8,9] As a common structural pattern, most of these clusters feature several gold(I) triphenylphosphine moieties AuL (with L = $P(C_6H_5)_3$) around a main-group element X_m (see Figure 1) although some unusual coordinations have also been found, e.g. the square pyramidal complex $\{[P(C_6H_5)_3Au]_4As\}^+$.[3] Strong efforts are being made[1] to complete this series of the general formula $[(LAu)_nX_m]^{(n+m-6)+}$ with respect to the central atoms X_m from the groups III to V (m = 1, 2, 3, respectively) or to extend the series to even higher coordination numbers. A tabular survey of the presently known clusters (see Table 1) exhibits an "island of stability" along its diagonal, i.e. an approximate correlation between the charge of the cluster cations and the number of AuL units.

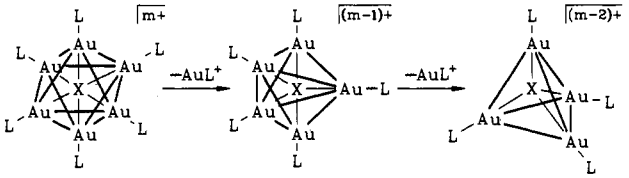

Figure 1. Decomposition of the octahedral cluster cations into their lower coordinate trigonal bipyramidal and tetrahedral analogues by successive loss of AuL^+ units (X_1 = B, X_2 = C, X_3 = N).

Table 1. Known n-Coordinate Main-Group Element-Centered Gold Clusters of the Form $[(LAu)_nX_m]^{(n+m-6)+}$ with L = PPh_3[a]

coordination number	cluster charge [(n+m−6)+]			
	0	1+	2+	3+
1	Cl[b]			
2	Se[c]	Cl[d]		
3		O,[e] S,[f] Se[f]		
4		N,[g] As[h]	O[i]	
5		C[j]	N,[k] P[l]	
6			C[m]	N[n] (?), P[o]

[a] The corresponding central atoms X_m are displayed. $X_1 \in$ group III, $X_2 \in$ group IV, $X_3 \in$ group V, $X_4 \in$ group VI, $X_5 \in$ group VII. [b] Reference 10. [c] Reference 11. [d] Reference 12. [e] Reference 13. [f] Reference 14. [g] Reference 2. [h] Reference 3 (quadratic pyramidal structure C_{4v}). [i] Reference 8. [j] Reference 4. [k] Reference 5. [l] Reference 6. [m] Reference 7. [n] Reference 15, but see also the comments in ref 6 and 8. [o] References 8 and 9.

In the present work we investigated the electronic structure and the stability of a variety of element-centered gold phosphine clusters and have focused on the isoelectronic series of six-coordinate clusters $[(LAu)_6X_m]^{m+}$ (X_1 = B, X_2 = C, X_3 = N). Only the carbon-centered member of this series has been synthesized so far; the existence of the nitrogen-centered cluster[15] is still under discussion.[6,8] To further probe the arguments put forward in this quantum chemical analysis, we have also applied the same line of reasoning to the four- and five-coordinate clusters, arriving finally at a rationalization of the "island of stability".

* Author to whom correspondence should be addressed.
† Lehrstuhl für Theoretische Chemie.
‡ Anorganisch-Chemisches Institut.
® Abstract published in *Advance ACS Abstracts*, August 1, 1994.

(1) Schmidbaur, H. *Gold Bull.* **1990**, *23*, 11.
(2) Slovokhotov, Y. L.; Struchkov, Y. T. *J. Organomet. Chem.* **1984**, *277*, 143.
(3) Zeller, E.; Beruda, H.; Kolb, A.; Bissinger, P.; Riede, J.; Schmidbauer, H. *Nature* **1991**, *352*, 141.
(4) Scherbaum, F.; Grohmann, A.; Müller, G.; Schmidbaur, H. *Angew. Chem., Int. Ed. Engl.* **1989**, 28, 463.
(5) Grohmann, A.; Riede, J.; Schmidbaur, H. *Nature* **1990**, *345*, 140.
(6) Schmidbaur, H.; Weidenhiller, G.; Steigelmann, O. *Angew. Chem., Int. Ed. Engl.* **1991**, *29*, 433.
(7) Scherbaum, F.; Grohmann, A.; Huber, B.; Krüger, C.; Schmidbaur, H. *Angew. Chem., Int. Ed. Engl.* **1988**, *27*, 1544.
(8) Schmidbaur, H. *Pure Appl. Chem.* **1993**, *65*, 691.
(9) Zeller, E.; Schmidbaur, H. *J. Chem. Soc., Chem. Commun.* **1993**, 69.
(10) Schmidbaur, H.; Weidenhiller, G.; Steigelmann, O.; Müller, G. *Chem. Ber.* **1990**, *123*, 285.
(11) Jones, P. G.; Thöne, C. *Chem. Ber.* **1991**, *124*, 2725.
(12) Jones, P. G.; Sheldrick, G. M.; Uson, R.; Laguna, A. *Acta Crystallogr. B* **1980**, *36*, 1486.
(13) Nesmeyanov, A. N.; Perevalova, E. G.; Struchkov, Y. T.; Antipin, M. Y.; Grandberg, K. I.; Dyadchenko, V. P. *J. Organomet. Chem.* **1980**, *210*, 343.
(14) Lensch, C.; Jones, P. G.; Sheldrick, G. M. *Z. Naturforsch. B* **1982**, *37*, 944.
(15) Brodbeck, A.; Strähle, J. *Acta Crystallogr. A* **1990**, *46*, C–232.

0002-7863/94/1516-8241$04.50/0

The electronic structure of gold phosphine compounds has been previously studied in several quantum chemical investigations. Indeed, the six-coordinate carbon-centered cluster was originally predicted on the basis of extended Hückel calculations.[16] These calculations have recently been extended to include also the boron- and nitrogen-centered clusters.[17] However, one should keep in mind that a reliable quantitative evaluation of binding energies and bond lengths is not feasible in extended Hückel theory, particularly when stretching motions are of importance. Therefore, results obtained with this method will remain essentially of a qualitative nature. Relativistic pseudopotential Hartree–Fock calculations have been carried out on the bare clusters $[Au_6X_m]^{m+}$ (X_m = B, C, N)[18] with the aim to investigate the size of the metal cage for different central atoms. Since electron correlation and the ligand influence were neglected in that work, the results are of limited relevance for the present goal. For the four-coordinate clusters with N, P, and As as "central" atoms, relativistic pseudopotential Hartree–Fock calculations were performed[19] to elucidate the experimentally observed[3] structural change from tetrahedral (for N) to square pyramidal (for As) coordination. These calculations included correlation by second-order perturbation theory (MP2) as well as ligands modeled by phosphines. Fully relativistic Dirac–Slater discrete-variational (DS-DV) Xα calculations have been performed[20,21] on the ligated clusters using phosphines as model ligands. A central result of this investigation, which is at variance with previous models for bonding in gold cluster compounds, is the participation of gold 5d orbitals in the metal–metal bonding, similar to the d^{10}–d^{10} interaction suggested earlier for Cu(I)–Cu(I)[22] and Pt(0)–Pt(0) complexes.[23] Via s–d hybridization this additional interaction mechanism, which is strongly enhanced by relativistic effects, leads to an interplay between radial X–Au and Au–L σ bonding on the one hand and the tangential gold–gold bonding on the other. Thus, for a proper description of the bonding in these element-centered gold cluster compounds it is essential to simultaneously take electron correlation, relativistic effects, and the influence of the ligands into account. At present, a reliable all-electron treatment of these systems by a "first principles" method seems to be only possible at the level of density functional theory.

Our previous work[20,21] using the DS-DV-Xα method focused on a molecular orbital analysis of octahedral gold cluster compounds but did not include a geometry optimization and the calculation of binding energies. The present investigation extends this work by means of an adequate electronic structure method, which is able to furnish geometries and binding energies, namely the quasirelativistic extension of the linear combination of Gaussian-type orbitals local density functional (R-LCGTO-LDF) method.[24–26]

We start our discussion by first describing the pertinent features of the R-LCGTO-LDF method as well as some computational details. Then we proceed to analyze the structural aspects of the ligand-free cluster cations. Topics of interest here are the effects of the charge on the cluster cations and the structural consequences of an atom in the center of the cluster as well as the extent of relativistic and electron correlation effects. In the next step, we investigate the influence of the phosphine ligands on the geometry and on the bonding of the cluster compounds. Then we present a detailed analysis of the energetic aspects that lead to the particular stability of the carbon-centered octahedral cluster. We put forth detailed arguments that the stabilizing effect of the ligands is most effective for positively charged clusters, although it competes with the increasing Coulomb repulsion within these cluster cations. In the last section we apply the concepts elaborated in an analysis of the lower coordinated clusters. We also investigate the stability of the cluster cations with respect to the loss of AuL^+ moieties, thus rationalizing the experimentally observed tendency of the lower coordinated clusters to aggregate further AuL^+ units. Here again the ligand influence turns out to be crucial.

2. Method and Computational Details

2.1. Quasirelativistic LCGTO-LDF Method. The quasirelativistic extension[24–26] of the LCGTO-LDF method[27,28] is based on the Douglas–Kroll (DK) transformation.[29] This transformation affords a variationally stable reduction of the four-component Dirac-type formalism to the familiar two-component formalism and permits the self-consistent treatment of relativistic effects. This methodology, based on the no-pair projection operator formalism of quantum electrodynamics, has been used previously in the context of wave-function-based electronic structure methods.[30–32]

We merely report the results of the DK transformation in the framework of the Kohn–Sham theory, correct to the second order in the effective one-particle potential v. One obtains[25,26] a set of two-component Kohn–Sham-like equations with an effective one-particle "Hamiltonian"

$$h_{KS}^{(2)} = E_p + A_p v A_p + A_p R_p v R_p A_p - \frac{1}{2}(E_p W^2 + W^2 E_p + 2W E_p W) \quad (1)$$

Here, the abbreviations

$$E_p = c(p^2 + c^2)^{1/2},\ A_p = \left(\frac{E_p + c^2}{2E_p}\right)^{1/2},\ R_p = \frac{c(\vec{\sigma}\cdot\vec{p})}{E_p + c^2} \quad (2)$$

have been used, where $\vec{\sigma}$ represents the vector of the Pauli spin matrices and $\vec{p}$ is the electronic momentum operator. The integral operator W is given in the momentum representation by

$$W_{p,p'} = A_p\left(\frac{R_p v_{p,p'} - v_{p,p'} R_{p'}}{E_p + E_{p'}}\right)A_{p'} \quad (3)$$

This type of transformation avoids the generation of highly singular operators that arise in the Foldy–Wouthuysen transformation.[33,34] As a consequence, matrix techniques[32] may be successfully employed for the evaluation of the various, rather complicated operators. However, only matrix elements of the operators $(\vec{p}\cdot v\vec{p})$ and $(\vec{p}\times v\vec{p})$ have to be evaluated in addition to those already required in the standard nonrelativistic version of the method. The latter matrix elements which are readily associated with the spin–orbit interaction are even needed in a scalar-relativistic variant of the method through cross terms that occur in the operator W^2 in eq 1.[26]

For the present investigation, the spin–orbit interaction is neglected. Furthermore, only the dominating nuclear potential is taken into account in the DK transformation but not the costly electronic contributions to the potential. Judging from atomic results,[24] one expects that most of the scalar-relativistic effects are taken into account by this level of theory (termed "vn2" in ref 26).

The scalar-relativistic density functional method described above has been successfully applied to the gold dimer,[26] to the series of mononuclear gold(I) complexes $(H_3C)Au(PR_3)$ with R = H, CH_3, and C_6H_5,[35] and to cerium bound endohedrally in C_{28}.[36,37] Judging from the results for

(16) Mingos, D. M. P. *J. Chem. Soc., Dalton Trans.* **1976**, 1163.
(17) Mingos, D. M. P.; Kanters, R. P. F. *J. Organomet. Chem.* **1990**, *384*, 405.
(18) Pyykkö, P.; Zhao, Y. *Chem. Phys. Lett.* **1991**, *177*, 103.
(19) Li, J.; Pyykkö, P. *Inorg. Chem.* **1993**, *32*, 2630.
(20) Rösch, N.; Görling, A.; Ellis, D. E.; Schmidbaur, H. *Angew. Chem., Int. Ed. Engl.* **1989**, *28*, 1357.
(21) Görling, A.; Rösch, N.; Ellis, D. E.; Schmidbaur, H. *Inorg. Chem.* **1991**, *30*, 3986.
(22) Mehrotra, P. K.; Hoffmann, R. *Inorg. Chem.* **1978**, *17*, 2187.
(23) Dedieu, A.; Hoffmann, R. *J. Am. Chem. Soc.* **1978**, *100*, 2074.
(24) Knappe, P.; Rösch, N. *J. Chem. Phys.* **1990**, *92*, 1153.
(25) Rösch, N.; Häberlen, O. D. *J. Chem. Phys.* **1992**, *96*, 6322.
(26) Häberlen, O. D.; Rösch, N. *Chem. Phys. Lett.* **1992**, *199*, 491.
(27) Dunlap, B. I.; Connolly, J. W.; Sabin, J. R. *J. Chem. Phys.* **1979**, *71*, 3396, 4993.
(28) Dunlap, B. I.; Rösch, N. *Adv. Quantum Chem.* **1990**, *21*, 317.
(29) Douglas, M.; Kroll, N. M. *Ann. Phys.* **1974**, *82*, 89.
(30) Sucher, J. *Phys. Rev. A* **1980**, *22*, 348.
(31) Almlöf, J.; Faegri, K.; Grelland, H. H. *Chem. Phys. Lett.* **1985**, *114*, 53.
(32) Hess, B. A. *Phys. Rev. A* **1986**, *33*, 3742.
(33) Foldy, L. L.; Wouthuysen, S. A. *Phys. Rev.* **1950**, *78*, 29.
(34) Moss, R. E. *Mol. Phys.* **1984**, *53*, 269.
(35) Häberlen, O. D.; Rösch, N. *J. Phys. Chem.* **1993**, *97*, 4970.
(36) Häberlen, O. D.; Rösch, N.; Dunlap, B. I. *Chem. Phys. Lett.* **1992**, *200*, 418.
(37) Rösch, N.; Häberlen, O. D.; Dunlap, B. I. *Angew. Chem., Int. Ed. Engl.* **1993**, *32*, 108.

Au_2,[26] one expects the local density approximation used here[38] to exhibit a tendency to overestimate binding energies.[39] This deficiency of the LDF method is acceptable in the present investigation, since we are mainly interested in changes of binding energies rather than in their absolute values. The scalar-relativistic version of the LCGTO-LDF method is computationally very efficient so that all-electron calculations are feasible even for the complexes $\{[(H_3C)_3PAu]_6X_m\}^{m+}$ with 85 atoms and more than 1600 contracted Gaussian-type MO basis functions.

2.2. Computational Details. Octahedral symmetry was assumed for the cluster core $[Au_6X_m]^{m+}$. The ligated model clusters $[(R_3PAu)_6X_m]^{m+}$ were calculated in idealized D_{3d} symmetry. The geometry optimizations of the present study focused on the distances from the gold atoms to the center of the cage and on the gold–ligand distances. These distances were varied in steps of 10 pm on a regular 5 × 5 grid. The bond lengths and force constants were determined by fitting a fourth-order Chebychev polynomial to the resulting energy values. The geometries of the various phosphine ligands were kept fixed. For PH_3, standard values were employed: $d(PH) = 141.5$ pm, $<(HPH) = 93.3°$.[40] In the case of $P(CH_3)_3$ the geometry determined experimentally in methyl(trimethylphosphine)-gold(I) was used: $d(PC) = 182.9$ pm, $<(CPC) = 103.2°$, $d(CH) = 107.8$ pm, and $<(HCH) = 108.0°$.[41]

Geometry optimizations as described above have been performed for all ligand-free octahedral cluster cores and for all element-centered octahedral clusters with simple phosphine ligands. For the empty clusters $[(H_3PAu)_6]^{m+}$ the geometry was optimized only for the charge $m = 2$ and used in the other calculations as well. The various gold complexes synthesized so far [1–9] feature triphenylphosphine ligands. These large ligands are much too costly to be used in the present electronic structure study. However, it has been shown that simple phosphine ligands PH_3 provide a satisfactory yet economical model for the investigation of structural aspects of such complexes.[35] On the other hand, adequate estimates of model binding energies can only be obtained with $P(CH_3)_3$ ligands.[35] Therefore, we recalculated the binding energies at the optimized geometries after replacing the simple phosphine ligands by trimethylphosphine ligands in order to obtain more reliable estimates for the (relative) cluster stabilities of experimental interest.

For the four- and five-coordinate cluster cations $[Au_4X_m]^{(m-2)+}$ (assumed T_d symmetry), $[Au_5X_m]^{(m-1)+}$ (D_{3d}), $[(H_3PAu)_4X_m]^{(m-2)+}$ (T_d), and $[(H_3PAu)_5X_m]^{(m-1)+}$ (C_{3h}), only the X–Au distances have been optimized, keeping the Au–P distances fixed as calculated in the corresponding six-coordinate clusters. In addition, in the five-coordinate clusters the axial and equatorial distances were constrained to be identical, an acceptable approximation as judged by the experimental values.[5] A possible distortion of the tetrahedral $[(LAu)_4N]^+$ into a quadratic pyramidal structure as in the case of $[(LAu)_4As]^+$ [3,19] has not been taken into account.

The orbital and fitting basis sets employed for Au, C, P, and H have been described previously.[35] The flexibility of the orbital basis set of the carbon atom in the center of the clusters was increased by adding a set of diffuse p functions, continuing the two most diffuse exponents in the fashion of a geometric series. The MO basis sets for the other central atoms, B and N, were constructed in analogous fashion. For a quick overview, the size of the uncontracted and general contracted basis sets used will be given in shorthand notation (for details see ref 35): Au (21s,17p,11d,7f)/[11s,10p,7d,3f]; B, C, and N as central atoms (9s,-6p,1d)/[7s,5p,1d]; C in the $P(CH_3)_3$ ligand (9s,5p,1d)/[7s,4p,1d]; P (12s,-9p,1d)/[8s,6p,1d]; H (6s,1p)/[4s,1p].

3. Results and Discussion

3.1. Structural Aspects of Clusters without Phosphine Ligands. The stability of the isoelectronic series of element-centered octahedral cluster cations $[(R_3PAu)_6X_m]^{m+}$ with X_1 = B, X_2 = C, and X_3 = N, has been rationalized using molecular orbital arguments (see Figure 2).[7,16,21] In this simplified view, one assumes that the Au 5d shell is closed and chemically inert and that the influence of the phosphine ligands does not have to be taken into account explicitly. Each Au atom (or rather each Au phosphine unit) contributes one valence orbital to the Au–X bonding, mainly a hybrid of Au 6s and 6p atomic orbitals. In

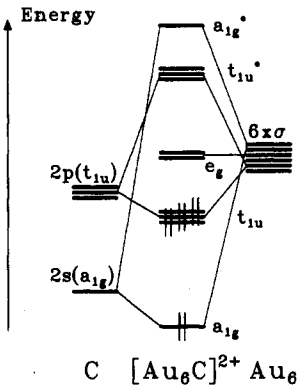

Figure 2. Schematic orbital interaction diagram for the carbon-centered octahedral cluster cation $[Au_6C]^{2+}$.

Table 2. Spectroscopic Constants (Bond Lengths d_{AuX}, Force Constants k_{AuX}, and Binding Energies ΔE) of the Empty Clusters $[Au_6]^{m+}$ (m = 0, ..., 4) and the Element-Centered Clusters $[Au_6X_m]^{m+}$ (X_1 = B, X_2 = C, X_3 = N)

	d_{AuX}[a] (pm)		k_{AuX} (N/m)		ΔE[d] (kJ/mol)	
system	nr[b]	rel[c]	nr	rel	nr	rel
Au_6	205	191	1.71	3.70	−913	−1289
$[Au_6]^{1+}$	206	191	1.62	3.77	−1043	−1504
$[Au_6]^{2+}$	208	191	1.36	3.68	−752	−1266
$[Au_6]^{3+}$	212	192	1.03	3.43	−62	−593
$[Au_6]^{4+}$	221	194	0.64	3.05	1028	523
$[Au_6B]^{1+}$	220	205	2.11	3.50	−621	−790
$[Au_6C]^{2+}$	223	204	1.98	3.21	−607	−666
$[Au_6N]^{3+}$	230	207	1.14	2.84	−372	−212

[a] For the empty clusters X refers to the center of the octahedron. [b] Nonrelativistic calculation. [c] Scalar-relativistic calculation. [d] Binding energies ΔE for $[Au_6]^{m+}$ are with respect to mAu$^+$ and $(6-m)$Au and for $[Au_6X_m]^{m+}$ are with respect to X_m and $[Au_6]^{m+}$.

octahedral symmetry, these six orbitals induce three sets of molecular orbitals (MOs), a_{1g}, t_{1u}, and e_g. The a_{1g} and t_{1u} levels favorably overlap with the s and p orbitals of the central main-group element X, respectively, and are completely filled by the eight valence electrons of the central cluster core (Figure 2).

In the "naked" cluster core Au_6, tangential metal–metal bonding dominates as strong radial bonds to the central atom are missing. The doubly occupied a_{1g} MO is the strongest binding MO and responsible for most of the cluster binding. The set of t_{1u} MOs, filled by four electrons, is mainly nonbonding, resulting in an open-shell electronic structure that may undergo a Jahn–Teller distortion.[42,43] Such a deviation from the ideal octahedral structure has probably little effect on the resulting bond distances and has not been taken into account in the present study. As can be seen from Table 2 a step-by-step removal of the four electrons in the t_{1u} MOs increases the nonrelativistic Au–Au bond length considerably. The corresponding gold-to-center distance lengthens by 16 pm from 205 to 221 pm, and the corresponding force constant decreases from 1.71 to 0.64 N/cm. On the other hand, in a relativistic calculation one encounters the well-known bond contraction[44] (by 14–25 pm) and a strong increase in the corresponding force constant. More noticeable is the reduced range of bond lengths (and also force constants) with the variation of the cluster charge. This means that in the relativistic case the bonding is strong enough to nearly compensate for the growing electrostatic repulsion due to the increasing charge of the cluster cation. For the empty clusters, this effect has to be attributed to relativistically enhanced metal–metal bonding.

Formal addition of a central atom (B, C, or N) to the Au_6 cluster results in an expansion of the cage, with the Au–X bond length increasing by about 15 pm. Thus the empty cage is too small to accommodate a guest atom without distortion. Here

(38) Vosko, S. H.; Wilk, L.; Nusair, M. *Can. J. Phys.* **1980**, *58*, 1200.
(39) Parr, R. G.; Yang, W. *Density Functional Theory for Atoms and Molecules*; Oxford University Press: New York, 1989.
(40) Weast, R. C., Ed. *CRC Handbook of Chemistry and Physics*, 64th ed.; CRC Press, Inc.: Boca Raton, FL, 1983.
(41) Haaland, A.; Hougen, J.; Volden, H. V. *J. Organomet. Chem.* **1987**, *325*, 311.
(42) Wales, D. J.; Mingos, D. M. P. *Inorg. Chem.* **1989**, *28*, 2748.
(43) Boča, R. *Czech. J. Phys.* **1990**, *40*, 629.
(44) Pyykkö, P. *Chem. Rev.* **1988**, *88*, 563.

again we notice the large range of the nonrelativistic bond lengths (220–230 pm) and the reduction of the force constant by nearly 50% (from 2.11 down to 1.14 N/cm). The radial bonds formed in the presence of a central atom are not strong enough to compensate for the geometric effect. In the relativistic case the cage expansion due to the central atom is rather similar, but again, the bond lengths and force constants change only slightly within the series of central atoms (205 → 207 pm and 3.50 → 2.84 N/cm).

It is not easy to isolate the effect of electron correlation in a density functional investigation.[39,45] To some extent this topic may be discussed by comparison to the results obtained from uncorrelated wave-function-based methods, i.e. to Hartree–Fock results. Such investigations for the unligated clusters $[Au_6X_m]^{m+}$ using quasirelativistic pseudopotentials yielded Au–X bond lengths of 220 pm for boron, 224 pm for carbon, and 235 pm for nitrogen.[18] These values resemble our nonrelativistic ones (see Table 2) but are at variance with our relativistic LCGTO-LDF results which range from 204 to 207 pm. Since a major difference between the two methods, HF and LDF, consists in the treatment of electron correlation this finding provides strong evidence that meaningful electronic structure investigations of gold cluster compounds have to include some treatment of correlation effects.

A comparison of the binding energies of the empty clusters (Table 2) shows that the stabilizing influence of relativistic effects ranges between about 380 and 530 kJ/mol. The absolute values are probably overestimated by the local density approach (LDA) used here.[39,46] An aspect often overlooked in a straightforward molecular orbital approach is the growing Coulomb repulsion within the cluster as the charge of the cluster cation increases. Both nonrelativistic and relativistic calculations show that the "naked" cluster cations are stable up to a charge of +3. However, if one takes the given overestimation of binding energies by the LDF method into account, one expects the cluster $[Au_6]^{3+}$ to probably be unstable with respect to the separated atoms. At both levels of theory, nonrelativistic and relativistic, the monocation $[Au_6]^+$ exhibits the largest binding energy. Since we did not aim at a complete structural characterization of the empty gold clusters, an octahedral symmetry constraint was imposed. Experimental[47] and theoretical[48] studies provide evidence that the gas-phase structure of the Au_6 and $[Au_6]^+$ clusters is a capped pentagon.

The s and p orbitals of the central atom which span a_{1g} and t_{1u} levels under O_h symmetry are ideally set up to overlap with the cage orbitals of the same irreducible representations, as is demonstrated by the high binding energies of the central atom to the empty gold cage (see Table 2). Boron is most strongly bound; nitrogen is bound weakest. This result confirms a previous analysis[21] which was based on overlap arguments. It was found that the overlap between the s and p orbitals of the central atom and the gold orbitals is least favorable for nitrogen, since its valence orbitals lie energetically low and are rather compact. Relativistic effects lead to a further increase in the binding energy for boron and carbon but to a decrease in the case of nitrogen. This at first sight unexpected effect may be connected to the reduced interaction between the low-lying nitrogen 2p orbitals and the relativistically destabilized Au 5d orbitals.[44]

3.2. Structural Aspects of Phosphine-Ligated Clusters. The influence of the triphenylphosphine ligands on the structure of the cluster compounds has been investigated theoretically in the corresponding phosphine analogues (see Table 3). The resulting gold–ligand bond lengths for the octahedral clusters fall in the range 227–224 pm and agree very well with the experimental bond distance of 227 pm for the carbon-centered cluster, a value which is quite typical for gold–phosphorus bonds.[49] The shortening of the Au–P bond and the strengthening of the corresponding force constant with increasing cluster charge meet the qualitative expectation for nucleophilic ligands. The values of 229 and 221 pm calculated for the Au–P bond lengths in $AuPH_3$ and $AuPH_3^+$, respectively, are bracketing the cluster values in a consistent fashion.

Before discussing the general effect of the ligands on the length of the Au–X bond, we would like to point out the small variation of this bond length found in the nonrelativistic calculations. The ligands cause a "quenching" of the range of Au–X bond distances just as relativistic effects do in the case of naked clusters. A rationalization of this finding may be derived from a model suggested previously[20,21] which invokes a participation of the gold 5d orbitals in the metal–metal bonding and correlates this contribution with the disruption of the formally closed $5d^{10}$ shell. The results of the present work support this model, as shown by the gold 5d populations displayed in Table 4. Mulliken populations should be reliable enough for the present purpose due to the compact nature of the Au 5d orbitals; this is confirmed by the comparison to the populations obtained previously in a DS-DV-Xα calculation which employs a minimal but optimized numerical basis.[20] Nonrelativistically the clusters without ligands have an almost closed $5d^{10}$ shell, whereas relativistic effects as well as the interaction with the phosphine ligands lead to a distinct reduction of the 5d population, both mechanisms contributing by a similar amount. The synergism of both effects results in a further decrease of the gold 5d population so that finally in the case of the relativistically treated ligated clusters the effective electronic configuration of gold is rather close to $5d^9$.

Octahedral clusters are synthesized from their lower coordinated descendants by addition reactions. Thus, we have calculated also the four- and five-coordinate element-centered cluster cations $[(LAu)_4X_m]^{(m-2)+}$ and $[(LAu)_5X_m]^{(m-1)+}$ (see Figure 1). Here we will focus on the Au–X bond only (Table 5, see also Section 2.2). The general effect of the ligands on the Au–X bond length is an average elongation by about 4 pm. This finding is in contrast to ab initio results[19] which yielded a shortening by 3–10 pm at the MP2 level in the cases of the four-coordinate clusters with N, P, and As as central atoms. However, the bond lengths

Table 3. Spectroscopic Constants (Bond Lengths and Force Constants) of the Ligated Clusters $[(H_3PAu)_6X_m]^{m+}$ (X_1 = B, X_2 = C, X_3 = N). Comparison of Results from Nonrelativistic (nr) and Relativistic (rel) Calculations

		d_{AuX}[b]		d_{AuP}[b]		k_{AuX}[c]		k_{AuP}[c]	
	system[a]	nr	rel	nr	rel	nr	rel	nr	rel
calc	$[(LAu)_6B]^+$	221	211	246	227	2.06	2.76	0.77	2.02
	$[(LAu)_6C]^{2+}$	219	208	244	226	1.97	2.99	0.93	2.21
	$[(LAu)_6N]^{3+}$	219	210	244	224	2.10	3.42	1.03	2.35
exp	$[(LAu)_6C]^{2+}$ [d]		212		227				
	$[(LAu)_6N]^{3+}$ [e]		213						

[a] Calculations for the model ligand L = PH_3; experimental values for L = PPh_3. [b] Bond lengths in pm. [c] Only diagonal force constants are displayed; values in N/cm. [d] Reference 7. [e] Reference 15, but see also the comment in ref 6.

Table 4. Gold 5d Mulliken Populations for the Clusters $[Au_6X_m]^{m+}$ and $[(LAu)_6X_m]^{m+}$ (X_1 = B, X_2 = C, X_3 = N) Comparing Results from Nonrelativistic (nonrel) and Relativistic (rel) Calculations

	nonrel with X_m =			rel with X_m =		
	B	C	N	B	C	N
$[Au_6X_m]^{m+}$ [a]	9.76	9.78 (9.72)	9.87	9.52	9.44 (9.53)	9.44
$[(LAu)_6X_m]^{m+}$ [a]	9.43	9.43 (9.45)	9.55	9.17	9.13 (9.29)	9.23

[a] This work with L = PH_3; values in parentheses for the carbon-centered clusters from a DS-DV-Xα calculation with L = SH_2.[20]

(45) Sabin, J. R.; Trickey, S. B. In *Local Density Approximations in Quantum Chemistry and Solid State Physics*; Dahl, J. P., Avery, J., Eds.; Plenum: New York, 1984.
(46) Ziegler, T. *Chem. Rev.* **1991**, *91*, 651.
(47) Taylor, K. J.; Jin, C.; Conceicao, J.; Wang, L.-S.; Cheshnovsky, O.; Johnson, B. R.; Nordlander, P. J.; Smalley, R. E. *J. Chem. Phys.* **1990**, *93*, 7515.
(48) Liao, D.-W.; Balasubramanian, K. *J. Chem. Phys.* **1992**, *97*, 2548.
(49) Schmidbaur, H. In *Gmelin Handbook of Inorganic Chemistry. Organogold Compounds*; Slawisch, A., Ed.; Springer Verlag: New York, 1980.

Table 5. Comparison of Spectroscopic Constants of the Gold-to-Central-Atom Bond for Four-, Five-, and Six-Coordinate Clusters

	$[Au_nX_m]^{(n+m-6)+}$ with X_m =			$[(LAu)_nX_m]^{(n+m-6)+}$ [a] with X_m =		
n	B	C	N	B	C	N
			d_{AuX}[b] (calc)			
4	198	192	193	203	198	198
5	202	199	201	204	203	204
6	205	204	207	211	208	210
			d_{AuX}[b] (exp)[c]			
4						202
5					208	209
6					212	213
			k_{AuX}[d] (calc)			
4	2.91	3.70	3.55	2.55	3.47	3.14
5	3.01	3.44	3.45	2.93	3.30	2.88
6	3.50	3.21	2.84	2.76	2.99	3.42

[a] L = PH_3. [b] Distance from the central atom to the gold atoms (average) in pm. [c] Experimental ligand L = PPh_3. References: $[(LAu)_4N]^+$, 2; $[(LAu)_5C]^+$, 4; $[(LAu)_5N]^{2+}$, 5; $[(LAu)_6C]^{2+}$, 7; $[(LAu)_6N]^{3+}$, 15, but see also the comment in ref 6. [d] Diagonal force constant for the gold-to-central-atom bond in N/cm.

obtained in these calculations are still too long by about 11 pm, compared to experiment.

In the LCGTO-LDF calculations, the carbon-centered clusters are found to have the shortest Au–X bond lengths for all coordinations although the differences compared to the boron- and nitrogen-centered clusters are small (Table 5). The increase of the Au–X bond length with increasing coordination number varies somewhat; the average is 5 pm per Au–L unit. Comparison to available experimental data shows that the Au–X bond lengths are slightly underestimated by the quasirelativistic LCGTO-LDF method (by ~4 pm). This may be interpreted as a manifestation of the overbinding often encountered in local density studies; see the findings for many organometallic compounds.[46] On the other hand, simple PH_3 ligands as models possibly lead to an underestimation of the Au–X distance if we generalize from the results found in the case of $MeAuPR_3$ (R = H, Me, Ph).[35] Taking into account this systematic underestimation, one may state that the trends in bond lenghts are predicted very well. Force constants are mainly reduced by the interaction of the ligands and the metal cluster core (Table 5), in line with expectations derived from the principle of bond order conservation.

Overall one notes that the results calculated for the cluster geometries confirm the picture established earlier based exclusively on the analysis of the molecular orbitals:[20,21] effects of the ligands, relativistic effects, and electron correlation together contribute to the strong bonding in the clusters.

3.3. Stability of the Octahedral Clusters. In the analysis presented so far nothing pointed toward a special role of carbon, perhaps with the exception of the fact that its clusters feature shorter Au–Au bond lengths than the "neighboring" B- and N-centered clusters. Experimentally the carbon-centered cluster is accessible with high abundance,[7] showing its exceptional stability. On the other hand, the existence of its nitrogen-centered analogue has been controversially discussed,[6,15] and the boron-centered cluster has, despite intense efforts, so far not been synthesized. To assess the stability of the clusters theoretically, we calculated fragment binding energies (as all-electron LDF total energy differences) in various ways.

In previous work the influence of the phosphine substituents on the gold–ligand bonding has been investigated for the series of gold(I) compounds $MeAuPR_3$ with R = H, Me, and Ph.[35] The model phosphine ligand turned out to be well suited for depicting structural aspects, as was again confirmed in the present work. However, models employing trimethylphosphine ligands are required if one aims at a nearly quantitative description of the energetic aspects of compounds with the triphenylphosphine ligands. Another finding of the previous study was the greatly enhanced affinity of the PR_3 group to the Au^+ ion (401 kJ/mol for PH_3, 553 kJ/mol for PMe_3, 580 kJ/mol for PPh_3) compared to the affinity to the neutral gold atom (124, 176, and 184 kJ/mol, respectively).

Table 6. Binding Energies (in kJ/mol) of the Ligands to the Naked Gold Cage, Empty or Element-Centered, and Binding Energy of the Central Atom to the Cage, Naked or Ligated[a]

educts	$m = 0$	$m = 1$	$m = 2$	$m = 3$	$m = 4$
$[Au_6]^{m+} + 6PH_3$	−794	−1084	−1500	−2038	−2666
$[Au_6]^{m+} + 6PMe_3$	−869	−1289	−1856	−2583	−3452
$[Au_6X_m]^{m+} + 6PH_3$		−1197	−1783	−2482	
$[Au_6X_m]^{m+} + 6PMe_3$		−1399	−2152	−3042	
$[Au_6]^{m+} + X_m$		−790	−666	−212	
$[(H_3PAu)_6]^{m+} + X_m$		−903	−949	−657	
$[(Me_3PAu)_6]^{m+} + X_m$		−900	−963	−672	

[a] The most stable clusters for each coordination are highlighted by underlining.

With this last result in mind, it is interesting to inspect the binding energy of the ligand shell to the gold core in the case of the octahedral cluster cations. As expected from this analogy, the affinity of the ligand shell to bind to the cluster core distinctly increases with the cluster charge (see Table 6). Replacement of the simple phosphine ligands by trimethylphosphine ligands enforces this trend, both for the element-centered and the empty cluster core. As an example, we analyze the ligand binding energies to the empty model clusters: the energy gained through the replacement of PH_3 by PMe_3 is just 75 kJ/mol for the neutral cluster but 786 kJ/mol for the hypothetical cluster with charge +4.

How does the presence of the central atom influence the ligand binding energies? Comparison of the data displayed in the first four rows of Table 6 shows that the central atom induces a further enhancement in the ligand binding energies. The binding energy *difference* between the clusters with charges $m = +3$ (nitrogen) and $m = +1$ (boron) is 954 and 1294 kJ/mol for the empty cages with L = PH_3 and PMe_3, respectively, but 1285 and 1643 kJ/mol for the element-centered clusters. Adding a central atom to the cage increases the ligand binding energy by 110 kJ/mol for boron, 296 kJ/mol for carbon, and 459 kJ/mol for nitrogen (all values for L = PMe_3). These trends also correlate with the electronegativity of the central atoms which may be responsible for a further increase of positive charge on the gold atoms, thereby leading to an even larger affinity of the ligands to the cage.

A complementary point of view on the energetics may be offered by directly comparing the binding energies of the central atom to the gold cage (see lower part of Table 6). In the case of the naked cage, a boron atom is favored, in agreement with orbital overlap arguments (see Section 3.1). On the other hand, the ligands induce a stronger radial bonding between the central atom and the gold cage which is most effective for nitrogen. This in turn leads to a preference of the ligated clusters for the carbon atom, although the difference compared to boron is small.

After having established the stabilizing effect of the ligands, we will consider the stability of the empty cage itself and how it is affected by its net charge. Table 7 shows the total binding energies of three series of empty cluster models both with and without ligands; also listed are the values for an octahedron of point charges. In each row of the table the most stable cluster is indicated by underlining. When going down the first four rows of Table 7, one notices a clear increase in the net charge carried by the most stable cluster of each row. To quantify this effect to a certain degree, we also display the (fractional) charge $\bar{m}$ for which the total energy assumes its minimum as determined by interpolating the values along each row.

For an arrangement of point charges only, the electrostatic repulsion obviously increases when proceeding along the row ($\bar{m}$ = 0.0). For the naked gold clusters this electrostatic repulsion is in most cases overcompensated for by the covalent gold–gold interaction; the singly charged cluster ($\bar{m}$ = 1.0) is the most stable

Table 7. Total Binding Energies[a] (in kJ/mol) of the Octahedral Empty and Element-Centered Clusters[d]

charge	$m = 0$	$m = 1$	$m = 2$	$m = 3$	$m = 4$	$\bar{m}$[b]
$[q_6]^{m+}$ [c]	0	202	808	1818	3232	0.0
$[Au_6]^{m+}$	−1289	−1504	−1266	−593	523	1.0
$[(H_3PAu)_6]^{m+}$	−2083	−2588	−2766	−2631	−2143	2.1
$[(Me_3PAu)_6]^{m+}$	−2159	−2793	−3121	−3176	−2928	2.7
$[Au_6X_m]^{m+}$		−2294	−1932	−805		1.0
$[(H_3PAu)_6X_m]^{m+}$		−3491	−3715	−3287		1.8
$[(Me_3PAu)_6X_m]^{m+}$		−3693	−4084	−3848		2.1

[a] Total binding energy with respect to the constituents X_m, mAu^+, $(6 - m)Au$, and $6PR_3$ (R = H, Me). [b] The value of m (as determined by a least squares fit to a parabola) for which the energy in the corresponding row assumes its minimum value. [c] Array of point charges (charge $q = +m/6$) in the geometry of $[Au_6]^{2+}$ (d_{qq} = 270 pm). [d] The most stable clusters for each coordination are highlighted by underlining.

one. The simple phosphine ligands further shift the position of maximum stability toward the dication ($\bar{m}$ = 2.1). This is a direct consequence of the previously discussed ability of the ligands to provide increasing stabilization for clusters with a higher net charge. Again, the trimethylphosphine ligands enhance this effect to furnish maximum stability for the cluster $[(Me_3PAu)_6]^{3+}$ ($\bar{m}$ = 2.7).

Formal addition of a central atom to the clusters shifts the position of maximum stability back to a lower net cluster charge (from $\bar{m}$ = 2.7 to $\bar{m}$ = 2.1) because the binding energy of the central atom is smallest for nitrogen (see Table 6). Thus, three main energy trends may be identified when one compares the various central atoms boron vs carbon vs nitrogen: the decreasing binding of the central atom to the cluster cage, the increasing electrostatic repulsion due to the compensating net cluster charge, and with a strong but opposite tendency, the improving ligand binding. All together, these counteracting effects produce a stability maximum for carbon in the center of an octahedral cluster.

Recently the structure and bonding in several pseudo-octahedral copper(I) cluster complexes has been investigated by the LCGTO-LDF method.[50] One of them, $[(Ph_3PCu)_6C]^{2+}$, as yet not synthesized, may be viewed as isoelectronic to the carbon-centered octahedral gold cluster. The total binding energy of the model compound $[(H_3PCu)_6C]^{2+}$, calculated by the same method as in the present work (see Section 2.2), amounts to 3570 kJ/mol[50] compared to 3715 kJ/mol for the corresponding gold cluster model compound. Thus, the copper cluster seems to be somewhat less stable. Most of the difference may be traced to the slightly lower ligand shell binding energy (reaction $[M_6C]^{2+} + 6PH_3 \rightarrow [(H_3PM)_6C]^{2+}$, M = Cu, Au) for copper (−1598 kJ/mol) than for gold (−1783 kJ/mol), as the total binding energy of the cluster core $[M_6C]^{2+}$ is quite comparable in both cases (Cu −1972 kJ/mol; Au −1932 kJ/mol).

3.4. Stability of the Lower Coordinated Clusters. As a final energetic aspect, we consider the stability of the gold phosphine compounds toward cluster fragmentation reactions. In the cases of the octahedral clusters, the possible loss of one or more AuL^+ moieties is of special interest. Figure 1 illustrates this process of cluster decomposition into lower coordinate clusters by two consecutive dissociation steps involving ligand dissociative losses of AuL^+ units. To study possible fragmentation reactions, calculations on the four-coordinate tetrahedral and five-coordinate trigonal bipyramidal cluster cations were performed. Only a restricted geometry optimization was performed (see Section 2.2 for details); however, the general conclusions to be reached below should not be affected by this approximation.

As a first step we analyze the fragmentation energies of the naked clusters. The energy changes in such reactions are compiled in Scheme 1, where a negative sign indicates an exoergic reaction. In some cases the release of a neutral Au atom instead of a cation Au^+ costs less energy and the corresponding values are given in brackets. There is a significant reduction in stability from boron to nitrogen, confirming the ordering of stability derived in previous extended Hückel calculations.[17] $[Au_6B]^+$ is stable with respect to the loss of an Au^+ ion, for $[Au_6C]^{2+}$ the energy change is about neutral, and $[Au_6N]^{3+}$ is thermodynamically unstable. Of course, the energy differences quoted provide no information about possible barriers along the reaction path.

The effect of phosphine ligands on the fragmentation energy will depend on the fact whether the ligands stabilize the educts better than the products or not. The corresponding energy changes for clusters with simple phosphine ligands (L = PH_3) are collected in Scheme 2. Again, the values in brackets characterize the energy changes in those cases where the loss of a neutral AuL moiety is more favorable. The phosphine ligands slightly lower the energy required to release a gold phosphine moiety from the boron-centered octahedral cluster, but a significant stabilizing effect is found in the clusters $[(LAu)_6C]^{2+}$ and $[(LAu)_6N]^{3+}$. In contrast to the situation without ligands, all three octahedral clusters are now stable with respect to the loss of one AuL^+ moiety.

Inspection of Scheme 2 reveals that only the five-coordinate nitrogen-centered cluster $[(LAu)_5N]^{2+}$ is unstable with respect to the loss of an AuL^+ moiety, to an even larger extent than the corresponding naked cluster. The reason for the instability of the latter cluster is the high average ligand binding energy of 280 kJ/mol per ligand in $[Au_4N]^+$ as compared to 254 kJ/mol per ligand in $[Au_5N]^{2+}$ (see Table 8). Thus, formal introduction of the phosphine ligands into the reaction $[Au_5N]^{2+} \rightarrow [Au_4N]^+ + Au^+$ leads to a stabilization of 252 (= 4 × 280 + 401 − 5 × 254) kJ/mol in favor of the products (the calculated Au^+ affinity of PH_3 is 401 kJ/mol[35]).

The energy change for the reaction $[(H_3PM)_4C] + 2MPH_3^+ \rightarrow [(H_3PM)_6C]^{2+}$ has recently been calculated for the case of copper (M = Cu), −843 kJ/mol.[50] This value is even larger than the corresponding one for M = Au (−768 kJ/mol). Thus, the hypothetical copper cluster $[(H_3PCu)_6C]^{2+}$ is more stable against fragmentation than the gold cluster $[(H_3PAu)_6C]^{2+}$ although the latter one has a somewhat higher total binding energy, as was discussed in Section 3.3. On the basis of these results, one would expect that there is a chance of synthesizing also the carbon-centered octahedral copper cluster.

Next we shall explore to which extent the various interaction mechanisms identified in the previous sections as influencing the stability of octahedral clusters may also be invoked to rationalize the energetics of the smaller cluster compounds. In Table 8 the binding energy of the ligand shell and the corresponding total binding energy of the clusters are displayed; both quantities are listed per ligand moiety to facilitate the comparison of the differently coordinated clusters. The correlation between the net cluster charge and the average binding energy per phosphine ligand is obvious. The ligand binding energy increases with the cluster charge. The upper right-hand subpanel of Table 8 features approximately constant values along the same diagonals as the upper left-hand subpanel. The calculated ligand binding energies range from 84 kJ/mol (for $[Au_4B]^-$) to 414 kJ/mol (for $[Au_6N]^{3+}$). This range is consistent with that calculated for the binding energies of PH_3 to Au (124 kJ/mol) on the one hand and to Au^+ (401 kJ/mol) on the other hand.[35]

In the lower left-hand subpanel of Table 8 the average total binding energies are displayed for the clusters *without* ligands; the values of the most stable clusters for each coordination number are underlined. The highest stability is found for the boron- and carbon-centered clusters. The relative stability of the nitrogen-centered clusters decreases with increasing coordination number. The situation changes significantly if one takes into account the stabilization offered by the phosphine ligand shell. The average total binding energy of the clusters *with* ligands, displayed in the lower right-hand subpanel of Table 8, may be obtained by adding the average ligand binding energies and the average binding energies of the naked clusters, i.e. the values from the lower left-

(50) Bowmaker, G. A.; Pabst, M.; Rösch, N.; Schmidbaur, H. *Inorg. Chem.* **1993**, *32*, 880.

Scheme 1

$$[Au_6X_m]^{m+} \xrightarrow{-Au^+} [Au_5X_m]^{(m-1)+} \xrightarrow{-Au^+} [Au_4X_m]^{(m-2)+} \quad 1$$

$\Delta E =$	537 kJ/mol (374)	$\Delta E =$ 945 kJ/mol (353)	$X_1 = B$
	55 kJ/mol	428 kJ/mol (280)	$X_2 = C$
	−434 kJ/mol	−63 kJ/mol	$X_3 = N$

Scheme 2

$$[(LAu)_6X_m]^{m+} \xrightarrow{-AuL^+} [(LAu)_5X_m]^{(m-1)+} \xrightarrow{-AuL^+} [(LAu)_4X_m]^{(m-2)+} \quad 2$$

$\Delta E =$	476 kJ/mol	$\Delta E =$ 1044 kJ/mol (601)	$X_1 = B$
	431 kJ/mol	337 kJ/mol (281)	$X_2 = C$
	356 kJ/mol	−315 kJ/mol	$X_3 = N$

Table 8. Comparison of Average Total Binding Energies per AuL Unit and Ligand-Shell Binding Energies for the Four-, Five-, and Six-Coordinate Clusters

	$[Au_nX_m]^{(n+m-6)+}$ with X_m =			$[(LAu)_nX_m]^{(n+m-6)+}$ [a] with X_m =		
n	B	C	N	B	C	N
	cluster charge			$\Delta E_{lig}/n$ [b]		
4	1−	0	1+	−84	−168	−280
5	0	1+	2+	−167	−197	−254
6	1+	2+	3+	−200	−297	−414
6[c]				−233[e]	−359[e]	−507[e]
		$\Delta E_{tot}/n$ [d]			$\Delta E_{tot}/n$ [d]	
4	−379	−363	−326	−463	−531	−606
5	−351	−375	−248	−518	−572	−502
6	−382	−322	−134	−582	−619	−548
6[c]				−616[e]	−681[e]	−641[e]

[a] L = PH_3. [b] Average binding energy of the ligands (in kJ/mol) to the cluster core. The left three columns contain the corresponding cluster charges to elucidate the relationship between the charges and the amount of stabilization through the ligand shell. [c] PMe_3 used as model ligand. [d] Average total binding energy per AuL unit (in kJ/mol) with respect to the fragments X_m, $(n + m - 6)Au^+$, $(6 - m)Au$, and (in the case of the ligated clusters) nL. In the case of $[Au_4B]^-$ the fragments B, Au^-, and 3Au were taken, accordingly in $[(LAu)_4B]^-$. The most stable clusters for each coordination are highlighted by underlining. [e] L = PMe_3.

hand and the upper right-hand subpanels. Obviously, the carbon- and nitrogen-centered ligated clusters feature the highest relative total stability. The effect is enhanced if one considers the more realistic ligands PMe_3 instead of the simple phosphine ligands PH_3.

After this analysis of the cluster binding the question arises whether the stability of the gold clusters is based mainly on radial Au–X bonds or on tangential Au–Au bonds. Formally, clusters of the type $[(LAu)_nX_m]^{(n+m-6)+}$ may be constructed by assembling closed-shell Au(I) units. The interaction between these units has been determined empirically to about 30 kJ/mol;[1,51,52] recent *ab initio* calculations at the MP2 level on the dimer $(ClAuPH_3)_2$ have confirmed this interaction.[53,54] The term "aurophilicity" has been coined[55] to describe this specific attraction. In a gold octahedron with its twelve Au–Au contacts, the aurophilic stabilization may thus be estimated to be about 360 kJ/mol. The resulting average stabilization energy per ligand of about 60 kJ/mol due to the tangential interaction between Au(I) units is quite small compared to the average total binding energy of about 600 kJ/mol in the case of the octahedral clusters, even if one takes into account that the calculated binding energies are overestimated by the LDA approach.[39,46] Due to this sizable difference between the total cluster binding energy and the aurophilic Au(I)–Au(I) interaction, the bonding in these element-centered gold clusters should be viewed as being of mainly radial nature between the gold phosphine units and the central atom.

Finally, we return to the "island of stability" in Table 1 which conveys the propensity of the main-group element-centered gold clusters to build up multiply charged cluster cations with increasing coordination around the central atom. From the common coordination numbers of the main-group elements and the isolobality of AuL units with hydrogen atoms, one would expect only the first two columns to be filled (partially) and the last two lines to be missing in the table. The approximately diagonal, extended shape of the filled fields in the table demonstrates the tendency to further aggregate $AuPR_3^+$ moieties; a clear manifestation is the uncommon sixfold coordination of carbon at the center of a gold phosphine cluster compound. The attractive aurophilic interaction between Au(I) units exhibiting the formal closed-shell configuration $5d^{10}$ certainly contributes to this phenomenon. However, an at least equally important stability aspect of these gold cluster cations is due to the balance between the increasing Coulomb repulsion within the cluster and the increasing stabilization of the cluster through the ligand shell of triphenylphosphines, the latter being most effective for higher charged clusters.

4. Summary and Conclusions

We have investigated the main-group element-centered octahedral gold cluster cations $[(R_3PAu)_6X_m]^{m+}$ ($X_1 = B$, $X_2 = C$, $X_3 = N$, and R = H, Me) by means of the scalar-relativistic version of the LCGTO-LDF method.[24-26] Geometry optimizations were performed for the naked clusters as well as for the phosphine-ligated clusters. The influence of the ligands on structural properties turned out to be moderate but nevertheless significant. The X–Au bond lengths were elongated on the average by about 4 pm; in the case of the carbon-centered cluster, a minimum for the X–Au bond length (208 pm) was found although the corresponding bond lengths for the two other clusters, with boron and nitrogen at the center, were quite similar. For a proper description of the electronic structure of these gold cluster compounds, relativistic effects, correlation effects, and ligand-induced effects are of similar importance, as judged from their influence on structural properties. The synergism of both relativistic effects and ligand influence leads to an opening of the formally closed Au $5d^{10}$ shell to an effective configuration of almost $5d^9$.

The phosphine ligands were found to exert a profound influence on the energetics of the various element-centered clusters. Among the unligated octahedral clusters, which have sometimes been studied as models of the ligated gold clusters, the boron-centered cluster is the most stable one. The nitrogen-centered cluster is by far the least stable one. Two main reasons have been identified

(51) Schmidbaur, H.; Graf, W.; Müller, G. *Angew. Chem., Int. Ed. Engl.* **1988**, *27*, 417.
(52) Jansen, M. *Angew. Chem., Int. Ed. Engl.* **1987**, *26*, 1098.
(53) Pyykkö, P.; Zhao, Y. *Angew. Chem., Int. Ed. Engl.* **1991**, *30*, 604.
(54) Li, J.; Pyykkö, P. *Chem. Phys. Lett.* **1992**, *197*, 586.
(55) Schmidbaur, H.; Scherbaum, F.; Huber, B.; Müller, G. *Angew. Chem., Int. Ed. Engl.* **1988**, *27*, 419.

for this observation: the less favorable radial overlap between the spatially rather contracted nitrogen s and p valence orbitals and the radially inward pointing gold cage hybrids as well as the strong electrostatic repulsion due to the largest net charge on the cluster. The formal addition of phosphine ligands to the cage reverses this energetic ordering, as the amount of stabilization is largest for the cationic clusters of the highest charge. The three ligated octahedral clusters exhibit a comparable net stability. The carbon-centered ligated cluster is the most stable one although the small relative energetic distance to the boron- and nitrogen-centered clusters does not preclude the possible existence of the latter ones. This hypothesis is further supported by the fact that all three clusters have been found stable with respect to the loss of an $AuPR_3^+$ moiety. A comparison of the total binding energies of the clusters with the empirically determined attractive mutual interaction between closed-shell Au(I) units points to a mainly radial bonding between the central atom and the $AuPR_3$ moieties.

The concept of increasing stabilization by phosphine ligands with increasing cluster charge carries over to the lower coordinated clusters where similar effects are observed. In this way, the clusters $[(AuL)_4N]^+$ and $[(AuL)_5C]^+$ were determined to be the most stable of the four- and five-coordinate systems, in agreement with the experimental experience gained so far.[2,4,5]

Acknowledgment. This work has been supported by the Deutsche Forschungsgemeinschaft through Sonderforschungsbereich 338 and by the Fonds der Chemischen Industrie.